SAND2022-15739C

DC Electrical Conductivity of Platinum From *Ab Initio* Simulation

Meghan K. Lentz[1,2], Joshua P. Townsend[2], and Kyle R. Cochrane[2]
[1]*Department of Physics, University of New Mexico, Albuquerque, NM, USA, and*
[2]*High Energy Density Physics Theory, Sandia National Laboratories, Albuquerque, NM, USA*

Platinum is a highly unreactive transition metal whose properties make it desirable for experiments at Sandia National Laboratories' Z Pulsed Power Facility (Z). In order to improve the use of platinum as a material standard in shock compression experiments, we investigated the necessary procedure to produce high quality DC electrical conductivity calculations from density functional theory using the Kubo Greenwood (KG) approximation. We studied the effects of changing several parameters involved in these calculations, all of which have some level of control over the calculated electrical conductivity. These parameters include the sampling of the Brillouin zone, smearing of the KG energy differences, the number of virtual orbitals included in the calculations, and the number of atomic configurations that are considered in the average electrical conductivity.

I. INTRODUCTION

Platinum is an unreactive metal with a high melting point whose face-centered cubic crystal does not display any experimentally observed phase changes up to melt. Due to these properties, platinum is frequently used as a material standard, particularly in high-pressure and shock compression physics [1]. For the experiments conducted at Sandia National Laboratories' (Sandia) Z Pulsed Power Facility (Z), it is important to understand material properties for a large portion of phase space. Experiments on Z are subjected to very large currents and magnetic fields, thus, understanding the electrical conductivity of materials being used as standards is important [2]. Current experimental diagnostics are often unable to diagnose the thermodynamic regimes relevant to Z, leading to a reliance on *ab initio* theory. In this study, we report the results of a systematic investigation of the DC electrical conductivity of platinum using density functional theory (DFT) and the Kubo Greenwood (KG) approximation. The quality of the estimate is sensitive to the approximations made both in the electronic structure and the numerical evaluation of the KG formula [3]. We show that in a modest supercell, one can obtain a robust well-converged estimate of the DC conductivity.

II. METHODS

In order to calculate the KG electrical conductivity, we first performed density functional theory based molecular dynamics (DFTMD) calculations. With the data from the DFTMD simulation we calculated the low energy electrical conductivity of platinum. We extrapolated the calculated conductivity to zero energy to obtain the DC conductivity. Electron-phonon coupling is accounted for by averaging the electrical conductivity over several atomic configurations.

A. Molecular Dynamic Simulations

The DFTMD calculations were conducted at 300K and ambient density, $\rho = 21.45\frac{g}{cm^3}$. Calculations were done using VASP, an implementation of Kohn-Sham DFT using periodic boundary conditions and a plane-wave basis [4–7]. The platinum $10e^-$ pseudopotential that was used has a $5d^9 6s^1$ valence configuration [8]. All simulations were conducted for a 108 atom cubic supercell within the NVT ensemble with a velocity scaling thermostat. The energy plane wave cutoff was set to 700 eV. The Brillouin zone was sampled at the Γ point. The exchange-correlation functional used is the Perdew-Burke-Ernzerhof (PBE) generalized gradient approximation [9]. The simulation was run for approximately 15,000 $1fs$ timesteps, and the energy and pressure were verified to be well-converged.

B. Electrical Conductivity Calculations

The essence of the KG formalism focuses on the physical interpretation of the single particle orbitals obtained from a Kohn-Sham DFT calculation. Within the KG approximation, the electrical conductivity, $\sigma_{\mathbf{k}}$, at frequency ω for a specific $\mathbf{k}$ point is given by:

$$\sigma_{\mathbf{k}}(\omega) = \frac{2\pi e^2\hbar^2}{3m^2\omega\Omega}\sum_{j=1}^{N}\sum_{i=1}^{N}\sum_{\alpha=1}^{3}[F(\epsilon_{i,\mathbf{k}}) - F(\epsilon_{j,\mathbf{k}})]\left|\langle\Psi_{j,\mathbf{k}}|\nabla_\alpha|\Psi_{i,\mathbf{k}}\rangle\right|^2\delta(\epsilon_{j,\mathbf{k}} - \epsilon_{i,\mathbf{k}} - \hbar\omega), \quad (1)$$

with e the charge of an electron, m the electron mass, Ω the cubic supercell volume element, and $F(\epsilon)$ the occupation from the Fermi-Dirac distribution [10]. The i and j indices sum over the N discrete bands included in the calculations and the α summation over the three spatial directions, respectively.

To calculate the electrical conductivity, we consider several atomic configurations from the DFTMD simulation. These atomic configurations must be statistically independent and are chosen based on an estimated correlation time, 128 fs, calculated from a block averaging of the energy. The conductivities for each snapshot are then averaged for the final electrical conductivity. Due to the low energy electrical conductivity's sensitivity to the Fermi surface, the chosen Brillouin zone sampling is crucial and looking only at the Γ point is no longer adequate.

The converged estimate of the low frequency portion of the electrical conductivity with respect to the investigated parameters is shown in Figure 1. Due to the finite size of the system, the lowest energy spectrum is plagued by finite size errors, evidenced by a drastic drop in the conductivity below approximately 0.01 eV. In order to capture the DC conductivity, we need to extrapolate the well resolved electrical conductivity to zero energy. Looking at Figure 1, showing the conductivity of the low energy region, the conductivity appears somewhat Drude-like. Therefore, we fit the KG results to the Drude model (Equation 2). It is important to exclude from the fit both the extremely low energy conductivities that are smaller than the typical eigenvalue separation, as well as the higher energy conductivities that have departed from a Drude-like curve.

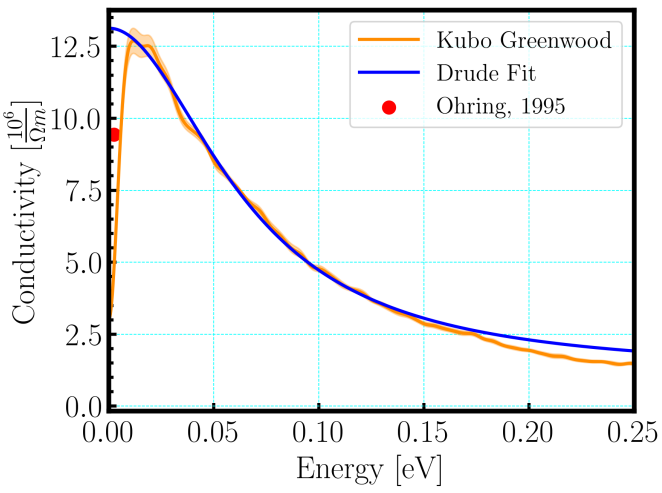

FIG. 1: Calculated Kubo Greenwood electrical conductivity for platinum at ambient conditions shown in orange with statistical error. The conductivity fit to the Drude model is shown in blue. The measured DC conductivity, $\sigma_{DC} = 9.43\frac{10^6}{\Omega m}$, is in red [11]. Sampled over a 10x10x10 irreducible wedge mesh with $\Delta = 0.004$ eV. Calculated using 10 snapshots and 800 total bands.

$$\sigma = \frac{\sigma_0}{1+\omega^2\tau^2} + constant. \quad (2)$$

A constant has been added to the form of the Drude model to ensure an optimal fit. From this fit, the DC conductivity can be reliably extrapolated. For the curve in Figure 1, $\sigma_0 = 12\frac{10^6}{\Omega m}$ and the constant term $1.2\frac{10^6}{\Omega m}$.

III. CONVERGENCE STUDIES

Accurately evaluating the KG electrical conductivity depends on several controllable parameters. We have studied these parameters to understand how best to represent the system. Included in these convergence studies are the **k** point mesh used to sample the Brillouin zone, the smearing term which smooths out local oscillations, the virtual orbitals included in the conductivity calculation, and the number of atomic configurations the electrical conductivity is averaged over.

A. Brillouin Zone Sampling

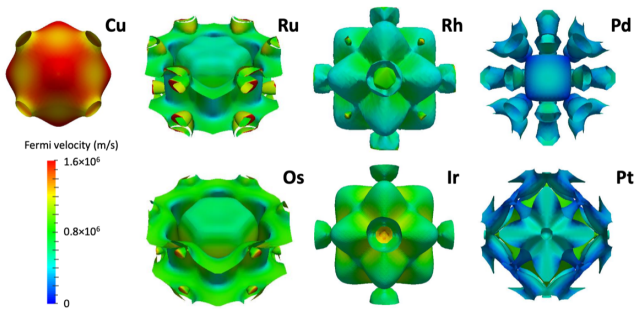

FIG. 4: Fermi surfaces of platinum-group metals. The Fermi surface of Cu is also shown as a reference. The color scheme indicates the Fermi velocity.

FIG. 2: Comparison of the Fermi surfaces for Pt-group metals. Note the dramatic difference in the complexity of the Fermi surface of platinum compared to that of copper. Image taken from Dutta, et al. (2017) [12].

The convergence of the Brillouin zone sampling is an essential step in the calculation of the electrical conductivity due to the extreme sensitivity of the DC conductivity to the **k** point mesh used. The number and location of the **k** points used determines where on the Fermi surface contributes to the conductivity calculation. For simple crystalline systems, such as copper and aluminum, which have nearly spherical Fermi surfaces, few **k** points are needed to sample the Fermi surface in order to sufficiently calculate the conductivity [10]. However, as seen in Figure 2 from Dutta, et al. (2017) [12], the Fermi surface of platinum is much more complex and, therefore, requires the use of more **k** points.

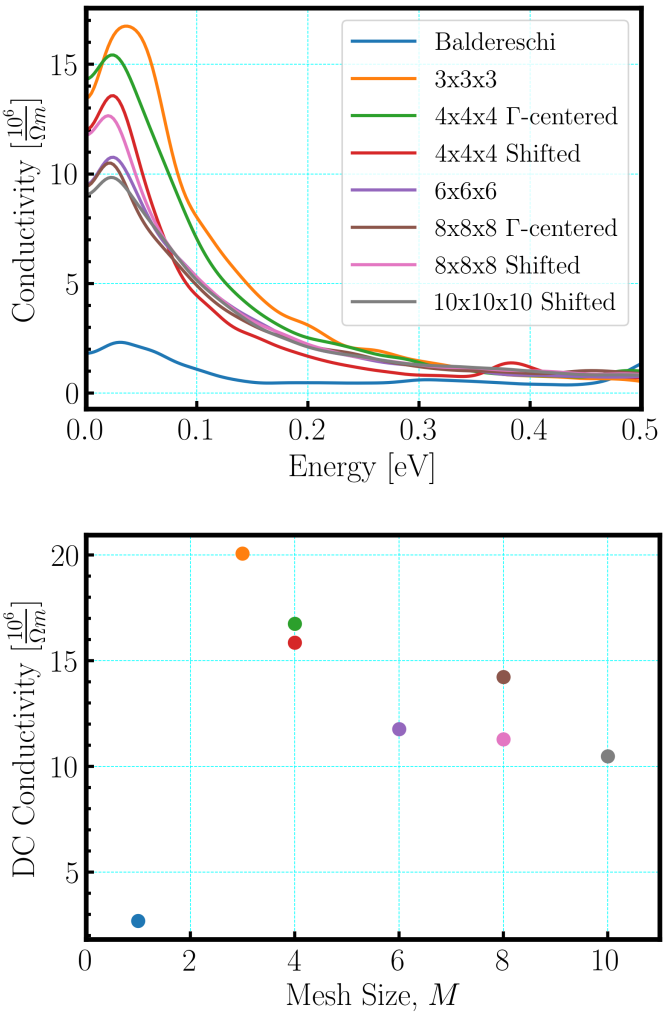

FIG. 3: Conductivity calculated for a range of **k** point grids (top panel). Calculated using a single snapshot with 800 total bands and $\Delta = 0.02$ eV. Corresponding DC conductivities extrapolated from Drude model fit (bottom panel).

For this study, we have sampled the 108 atom platinum system with meshes ranging from 1x1x1 to 10x10x10. The number of **k** points increase as M^3 for an MxMxM mesh causing the higher order meshes to become too computationally expensive, thus, we used the irreducible wedge for the samplings larger than a single **k** point. To do this, we give VASP an explicit set of **k** points for which we ignore the breaking of symmetries caused by thermal fluctuations and assume the full set of symmetries are present. We have considered both Γ-centered grids and the shifted Monkhorst-Pack scheme. In Figure 3, the electrical conductivities calculated using KG are shown for the different Brillouin zone samplings (top panel), as well as the extrapolated DC conductivities from the fit to the Drude model (bottom panel). For the sake of computation time, all conductivities are calculated using a single snapshot. To avoid bias, the same snapshot is used for each calculation. These results are looking only at the convergence of the DC conductivity with respect to the number of **k** points needed. From Figure 3, we see that the estimated electrical conductivity does not vary monotonically with respect to the number of **k** points. It is clear that a large number of **k** points are necessary to calculate a converged DC conductivity and that the spread in calculated conductivities is very large for the different **k** point meshes [3].

B. Discrete Band Structure Smearing

Another variable that has a large influence over the calculated electrical conductivity is the smearing of the discrete KG energies. Due to the finite simulation size, the δ function in Equation 1 needs to be broadened. This is done using a Gaussian broadening [9].

$$\delta(\epsilon_{j,\mathbf{k}} - \epsilon_{i,\mathbf{k}} - \hbar\omega) \rightarrow e^{-\frac{(\epsilon_{j,\mathbf{k}} - \epsilon_{i,\mathbf{k}} - \hbar\omega)^2}{2\Delta^2}}, \qquad (3)$$

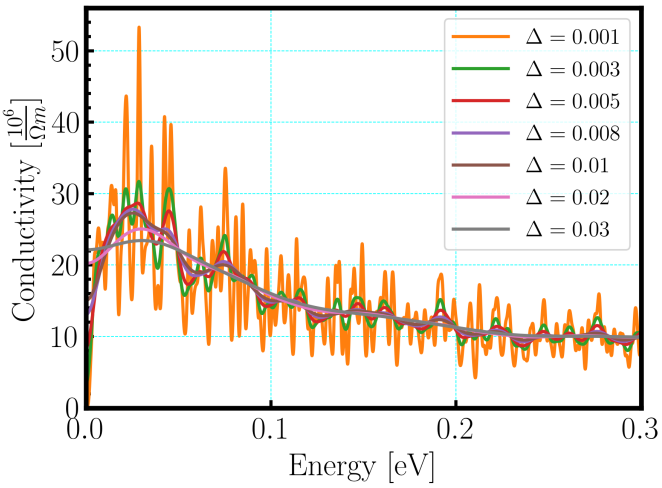

FIG. 4: Kubo Greenwood conductivity calculations with different levels of discrete band structure smearing. Calculations were sampled with a 4x4x4 shifted grid for expediency, using the irreducible wedge. Calculated from a single snapshot and 800 bands.

where Δ is the width of the Gaussian. Previous literature [10] has suggested taking Δ equal to the average difference in energy eigenvalues above and below the Fermi energy, weighted by the slope of the Fermi distribution as a starting point for finding the ideal smearing. It is suggested when choosing the amount of smearing to approach the eigenvalue spacing from below to prevent over smearing. For platinum, we have calculated the Fermi energy to be 11.1 eV with the average difference between eigenvalues approximately 0.02 eV. In Figure 4, we have

calculated the KG electrical conductivity of a single snapshot for a range of Δ.

Looking at Figure 4, large oscillations in the conductivity are the result of under smearing, and make robust estimation of the DC conductivity a challenge. As the smearing term increases, the KG conductivity in the figure becomes very smooth before flattening and losing its structure, which causes a notable drop in the extrapolated DC conductivity. Because it is necessary to avoid over smearing the conductivity, we preserve some minimal oscillations in the KG calculation. From this, we have determined the optimal width of the Gaussian to be between 0.003 eV, which maintains a larger degree of oscillations than necessary, and 0.005 eV, where the curve has been significantly smoothed and may be experiencing some structure loss.

C. Number of Orbitals

Included in VASP is the ability to choose the number of Kohn-Sham orbitals that contribute to the calculation. As a minimum, VASP requires all occupied states, plus one unoccupied band. Calculating the KG electrical conductivity for each **k** point, we sum over the number of orbitals in the system, thus, the inclusion of a large number of virtual orbitals is necessary. While empty bands do not contribute to the energy, they are essential to better represent real systems for conductivity calculations. A common way to check the quality of a calculated physical quantity is through the evaluation of sum rules. For a range of different sized systems, we have calculated the f-sum rule (Equation 4) [10]. It becomes clear in Figure 5 that the inclusion of a very large number of orbitals is necessary for the total KG electrical conductivity to converge. However, the additional higher energy bands are unoccupied and contribute very little to the low frequency conductivity.

$$S(\omega) = \frac{2m\Omega}{\pi e^2 N_e} \int_0^\infty \sigma(\omega) d\omega = 1 \tag{4}$$

In addition to our sum rule calculations, we also extrapolated the DC conductivities for systems of varying sizes, finding that the DC conductivity does not change for the range of 800 to 2000 bands. For the purposes of this work, we are interested in finding the DC conductivity of our system, looking only at the low energy conductivity, between 0.0-0.5eV. Due to this, we require fewer virtual orbitals without the convergence of the sum rule. We have included approximately 800 total bands, greatly decreasing computation times.

D. Number of Snapshots

Lastly, we ran calculations looking at the necessary number of atomic configurations to be included in the conductivity calculation. By averaging the conductivity calculation over a number of different atomic configurations, we are able to capture the effects of electron-phonon coupling. Snapshots were taken from the end of the DFTMD ambient calculation to ensure equilibration. The KG electrical conductivity was then calculated including 1, 5, 10, 15, and 19 snapshots. From Figure 6, it is clear that considering only a single atomic configuration is not representative of the converged KG conductivity; however, a rather small number of configurations (10) is sufficient to see the system converge with relatively small error.

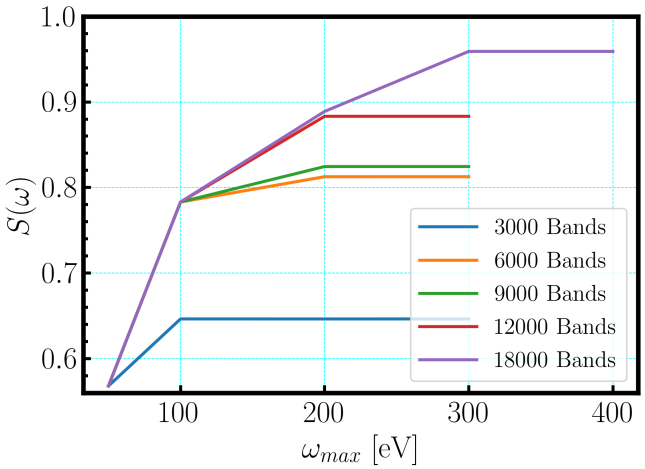

FIG. 5: f-sum rule calculations increasing the maximum energy difference required for excitation pairs to be included in conductivity calculations. The DC conductivity remains the same as the size of the system decreases to 800 bands. The different lines represent different sized systems of discrete Kohn-Sham orbitals.

IV. REMARKS AND FUTURE WORK

In Figure 1, we have combined all of the findings from the convergence studies in order to determine the DC conductivity for platinum at ambient conditions. For this calculation, the number of energy points where the conductivity is calculated is 40,000 and the number of bands 800. The Brillouin zone is sampled using the shifted 10x10x10 irreducible wedge, Δ is set to 0.004 eV, and we have averaged over 10 snapshots. This work has not yet accounted for the finite simulation size. The calculated Drude DC conductivity for this calculation is $13.1 \frac{10^6}{\Omega m}$, which is within 28% of the measured value $9.43 \frac{10^6}{\Omega m}$. This level of error is not uncommon for calculations of the DC electrical conductivity using the KG approximation. Previous literature reports errors of up to 30% [10] and up to 50% [3].

This method of calculating the electrical conductivity has shown great success in studying many different sys-

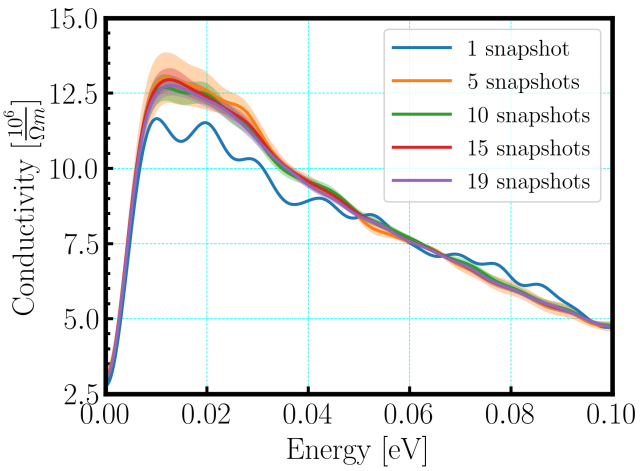

FIG. 6: Kubo Greenwood conductivities calculated with contributions from a varying number of atomic configurations, including statistical error. Calculated including 800 bands sampled with a 10x10x10 shifted mesh and $\Delta = 0.004$ eV.

tems, particularly those in the hot dense regime [3, 13], however, it does have its limitations. Although DFT is in principle an exact theory, the exact functional is unknown. Therefore, approximate forms are used, which introduce systematic inaccuracies difficult to quantify.

In summary, we have shown that the successful calculation of the DC electrical conductivity using the KG approximation requires a level of fine tuning. The calculated electrical conductivity is highly dependent on the sampling of the Brillouin zone, especially for materials like platinum with a complex Fermi surface. Applying sufficient smearing to the KG electrical conductivity is also vital in reducing the amount of noise in the low energy region. Conversely, applying too much smearing results in the flattening of the conductivity curve, causing the calculated DC electrical conductivity to drop substantially. We have also shown that convergence of the full optical conductivity is not necessary when interested in only the low energy electrical conductivity. Capturing the electron-phonon coupling does require the calculation of more than one atomic configuration; however, a relatively small number of configurations is suitable for calculating the KG electrical conductivity.

V. ACKNOWLEDGEMENTS

We would like to thank Mike Desjarlais for many helpful discussions. Sandia National Laboratories is a multimission laboratory managed and operated by National Technology & Engineering Solutions of Sandia, LLC, a wholly owned subsidiary of Honeywell International Inc., for the U.S. Department of Energy's National Nuclear Security Administration under contract DE-NA0003525. This paper describes objective technical results and analysis. Any subjective views or opinions that might be expressed in the paper do not necessarily represent the views of the U.S. Department of Energy or the United States Government.

[1] K. R. Cochrane, P. Kalita, J. L. Brown, C. A. McCoy, J. W. Gluth, H. L. Hanshaw, E. Scoglietti, M. D. Knudson, S. P. Rudin, and S. D. Crockett, Phys. Rev. B **105**, 224109 (2022).

[2] D. B. Sinars, M. A. Sweeney, C. S. Alexander, D. J. Ampleford, T. Ao, J. P. Apruzese, C. Aragon, D. J. Armstrong, K. N. Austin, T. J. Awe, A. D. Baczewski, J. E. Bailey, K. L. Baker, C. R. Ball, H. T. Barclay, S. Beatty, K. Beckwith, K. S. Bell, J. F. Benage, Jr., N. L. Bennett, K. Blaha, D. E. Bliss, J. J. Boerner, C. J. Bourdon, B. A. Branch, J. L. Brown, E. M. Campbell, R. B. Campbell, D. G. Chacon, G. A. Chandler, K. Chandler, P. J. Christenson, M. D. Christison, E. B. Christner, R. C. Clay, III, K. R. Cochrane, A. P. Colombo, B. M. Cook, C. A. Coverdale, M. E. Cuneo, J. S. Custer, A. Dasgupta, J. P. Davis, M. P. Desjarlais, D. H. Dolan, III, J. D. Douglass, G. S. Dunham, S. Duwal, A. D. Edens, M. J. Edwards, E. G. Evstatiev, B. G. Farfan, J. R. Fein, E. S. Field, J. A. Fisher, T. M. Flanagan, D. G. Flicker, M. D. Furnish, B. R. Galloway, P. D. Gard, T. A. Gardiner, M. Geissel, J. L. Giuliani, M. E. Glinsky, M. R. Gomez, T. Gomez, G. P. Grim, K. D. Hahn, T. A. Haill, N. D. Hamlin, J. H. Hammer, S. B. Hansen, H. L. Hanshaw, E. C. Harding, A. J. Harvey-Thompson, D. Headley, M. C. Herrmann, M. H. Hess, C. Highstrete, O. A. Hurricane, B. T. Hutsel, C. A. Jennings, O. M. Johns, D. Johnson, M. D. Johnston, B. M. Jones, M. C. Jones, P. A. Jones, P. E. Kalita, R. J. Kamm, J. W. Kellogg, M. L. Kiefer, M. W. Kimmel, P. F. Knapp, M. D. Knudson, A. Kreft, G. R. Laity, P. W. Lake, D. C. Lamppa, W. L. Langston, J. S. Lash, K. R. LeChien, J. J. Leckbee, R. J. Leeper, G. T. Leifeste, R. W. Lemke, W. Lewis, S. A. Lewis, G. P. Loisel, Q. M. Looker, A. J. Lopez, D. J. Lucero, S. A. MacLaren, R. J. Magyar, M. A. Mangan, M. R. Martin, T. R. Mattsson, M. K. Matzen, A. J. Maurer, M. G. Mazarakis, R. D. McBride, H. S. McLean, C. A. McCoy, G. R. McKee, J. L. McKenney, A. R. Miles, J. A. Mills, M. D. Mitchell, N. W. Moore, C. E. Myers, T. Nagayama, G. Natoni, A. C. Owen, S. Patel, K. J. Peterson, T. D. Pointon, J. L. Porter, A. J. Porwitzky, S. Radovich, K. S. Raman, P. K. Rambo, W. D. Reinhart, G. K. Robertson, G. A. Rochau, S. Root, D. V. Rose, D. C. Rovang, C. L. Ruiz, D. E. Ruiz, D. Sandoval, M. E. Savage, M. E. Sceiford, M. A. Schaeuble, P. F. Schmit, M. S. Schollmeier, J. Schwarz, C. T. Seagle, A. B. Sefkow, D. B. Seidel, G. A. Shipley, J. Shores, L. Shulenburger, S. C. Simpson, S. A. Slutz, I. C. Smith, C. S. Speas, P. E. Specht, M. J. Speir, D. C. Spencer, P. T. Springer, A. M. Steiner, B. S. Stoltzfus,

W. A. Stygar, J. Ward Thornhill, J. A. Torres, J. P. Townsend, C. Tyler, R. A. Vesey, P. E. Wakeland, T. J. Webb, E. A. Weinbrecht, M. R. Weis, D. R. Welch, J. L. Wise, M. Wu, D. A. Yager-Elorriaga, A. Yu, and E. P. Yu, Physics of Plasmas **27** (2020), 10.1063/5.0007476.

[3] M. Pozzo, M. P. Desjarlais, and D. Alfè, Phys. Rev. B **84**, 054203 (2011).

[4] G. Kresse and J. Hafner, Phys. Rev. B **47**, 558 (1993).

[5] G. Kresse and J. Hafner, Phys. Rev. B **49**, 14251 (1994).

[6] G. Kresse and J. Furthmüller, Phys. Rev. B **54**, 11169 (1996).

[7] G. Kresse and J. Furthmüller, Computational Materials Science **6**, 15 (1996).

[8] (10Mar2009), the POTCAR file used was PAW_PBE Pt_GW.

[9] J. P. Perdew, K. Burke, and M. Ernzerhof, Phys. Rev. Lett. **77**, 3865 (1996).

[10] M. P. Desjarlais, J. D. Kress, and L. A. Collins, Phys. Rev. E **66**, 025401 (2002).

[11] M. Ohring, *Engineering materials science* (Academic Press, 1995).

[12] S. Dutta, K. Sankaran, K. Moors, G. Pourtois, S. V. Elshocht, J. Bommels, W. Vandervorst, Z. Tokei, and C. Adelmann, Journal of Applied Physics **122**, 025107 (2017).

[13] A. Kietzmann, B. Holst, R. Redmer, M. P. Desjarlais, and T. R. Mattsson, Phys. Rev. Lett. **98**, 190602 (2007).